

Highly Red Emissive Conjugated Homopolymers Based on Double B←N Bridged Bipyridine Unit

Yu-Yue Gao^{a,b}, Kai-Yuan Zhang^{a,b}, Shu-Meng Wang^a, Hui Tong^{a,b}, and Jun Liu^{a,b*}^a State Key Laboratory of Polymer Physics and Chemistry, Changchun Institute of Applied Chemistry, Chinese Academy of Sciences, Changchun 130022, China^b School of Applied Chemistry and Engineering, University of Science and Technology of China, Hefei 230026, China Electronic Supplementary Information

Abstract Conjugated homopolymers based on six-member rings, *e.g.*, polyfluorene, always exhibit blue emission and conjugated homopolymers based on five-member rings, *e.g.*, polythiophene, can give red emission with low efficiency. In this work, we report a series of new conjugated homopolymers based on six-member rings with high-efficiency deep-red emission. The repeating units of the red light emitting homopolymers are double B←N bridged bipyridine (BNBP) with the boron atoms functionalized with diphenyl, borafuorene, and 2,7-di-*tert*-butyl-borafuorene groups, respectively. The relationship between the chemical structures and the opto-electronic properties of the monomers and the homopolymers has been systematically studied. The three polymers emit pure red light (λ_{\max} =656 nm) or deep red light (λ_{\max} =693 nm) with fluorescence quantum efficiency in solution higher than 60%. The polymers can be used as the emitters in solution-processed organic light-emitting diodes with red emission and decent device performance. This work indicates a new strategy to design highly efficient light emitting conjugated polymers.

Keywords Conjugated homopolymers; Double B←N bridged bipyridine (BNBP); Deep-red emission; High fluorescent efficiency

Citation: Gao, Y. Y.; Zhang, K. Y.; Wang, S. M.; Tong, H.; Liu, J. Highly red emissive conjugated homopolymers based on double B←N bridged bipyridine unit. *Chinese J. Polym. Sci.* <https://doi.org/10.1007/s10118-024-3123-7>

INTRODUCTION

Conjugated polymers are an important kind of opto-electronic materials with the great advantages of flexibility, solution processing with low cost.^[1–5] In particular, carefully designed conjugated polymers exhibit excellent light emitting properties and can be used as active layer in high performance organic light-emitting diodes (OLEDs).^[6–16] To elucidate the relationship between chemical structures and light emitting properties of conjugated polymers, homopolymers are ideal model compounds. Conjugated homopolymers based on six-member rings, *e.g.*, polyfluorene, always exhibit wide bandgap with blue emission and high fluorescence efficiency.^[17–23] In comparison, conjugated homopolymers based on five-member rings, *e.g.*, polythiophene, generally exhibit medium bandgap with red emission and always show low fluorescence quantum efficiency.^[24–27] In this work, for the first time, we report a series of new conjugated homopolymers based on six-member rings with high-efficiency deep-red emission.

In 2016, we developed an organoboron building block, double B←N-bridged bipyridine (BNBP), which can be used to design n-type polymer semiconductors with low-lying en-

ergy levels and high electron mobilities.^[28] These BNBP-based conjugated polymers have been used as active layers in high-performance organic solar cells (OSCs),^[29–31] organic field-effect transistors (OFETs),^[32] organic thermoelectrics (OTEs),^[33] organic photodetectors (OPDs)^[34] and metal-free electrocatalyst (MFEC) for oxygen reduction.^[35] Most of these BNBP-based conjugated polymers are alternating copolymers. The opto-electronic properties and opto-electronic device applications of BNBP-based homopolymers are rarely studied.

Herein, by introducing large steric hindrances to the two boron atoms of BNBP, we develop a series of BNBP building blocks based on six-membered rings with non-planar configuration. The resulting conjugated homopolymers exhibit deep-red emission with high fluorescence quantum efficiencies (Φ_F =*ca.* 0.6). The relationship between the chemical structures of the BNBP building blocks and the opto-electronic properties of the conjugated homopolymers has been systematically studied. The application of these conjugated homopolymers in solution-processed OLEDs has also been demonstrated.

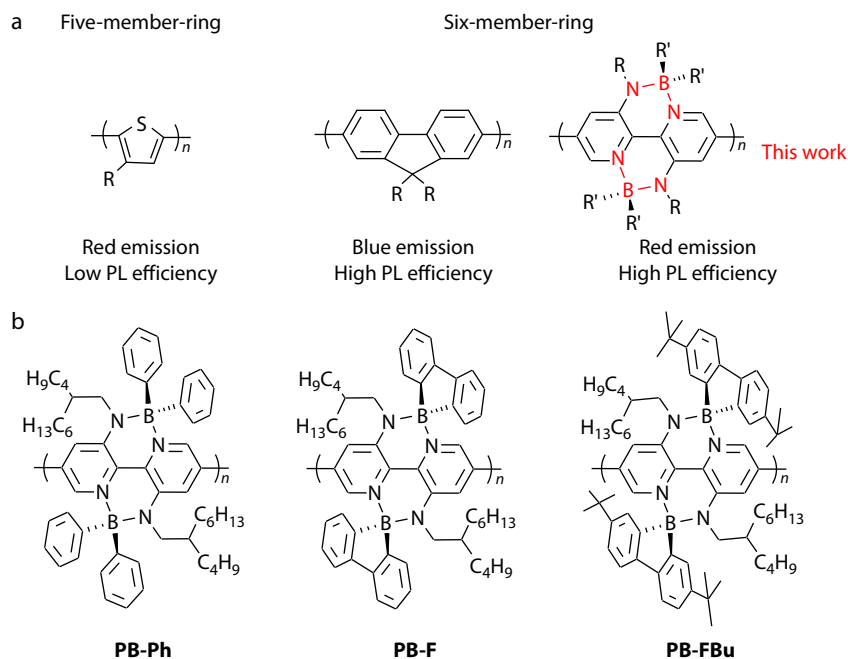
EXPERIMENTAL

Molecular Design

Scheme 1 (b) shows the chemical structures of the three conjugated homopolymers, **PB-Ph**, **PB-F** and **PB-FBu**. In the building

* Corresponding author, E-mail: liujun@ciac.ac.cn

Received January 28, 2024; Accepted March 11, 2024; Published online April 25, 2024



Scheme 1 (a) Schematic illustration of homopolymer examples; (b) Chemical structures of designed polymer **PB-Ph**, **PB-F** and **PB-FBu**.

blocks of the three homopolymers, the B atoms are functionalized with two phenyl units, fluorene unit, and di(*tert*-butyl)fluorene unit, respectively. To study the configuration and electronic structure of the BNPB building blocks, we performed density functional theory (DFT) calculations at the B3LYP/6-31G(d,p) level of the three di-bromo monomers, **mB-Ph**, **mB-F** and **mB-FBu** (see Fig. 1). The long and branched alkyl side chains have been replaced by methyl for simplified DFT calculations. Fig. 1 shows the optimized molecular geometries and the lowest unoccupied molecular orbitals (LUMO)/highest occupied molecular orbitals (HOMO) of the three monomers. All the three monomers exhibit non-planar configurations. In **mB-Ph**, the dihedral angles of the two phenyl units and the BNPB unit are 62.5° and 86.3°, respectively. In comparison, in **mB-F**, the borafluorene unit adopts perpendicular configuration with the BNPB unit with a dihedral angle of 90°. The steric hindrance effect of the borafluorene unit is larger than that of the two phenyl units. The *tert*-butyl groups on the borafluorene unit in **mB-FBu** should further increase the steric hindrance effect of the substitutes of the boron atoms. The LUMOs of the three monomers are distributed on the bipyridine unit. The HOMO of **mB-Ph** is mainly distributed on the bipyridine unit and is not distributed on the diphenyl unit. In comparison, in **mB-F**, the HOMO is distributed on both the bipyridine unit and the borafluorene unit. This indicates that the substitutes on the boron atom should affect the HOMO energy levels of the building blocks. In addition, the *tert*-butyl groups with electron-donating property should also affect the HOMO energy levels of **mB-FBu**. As shown in Figs. S2 and S3 (in the electronic supplementary information, ESI), the backbones of the three homopolymers all exhibit twisted conformation with the optimized dihedral angle between two adjacent BNPB units of ca. 33°. The aromatic substituents on the B atoms act as steric hindrances to suppress intermolecular interaction of the three homopolymers in the solid state. The LUMOs of the three polymers are well delocalized over the polymer

backbone and the HOMOs of the three polymers are mainly localized on one BNPB unit. Such delocalized LUMO and localized HOMO are always observed for BNPB-based conjugated polymers reported previously.

Synthesis

Synthesis of **mB-F**

5,5'-Dibromo-*N*³,*N*³-bis(2-butyloctyl)-[2,2'-bipyridine]-3,3'-diamine (1) (681 mg, 1.0 mmol) and triethylamine (405 mg, 4.0 mmol) were combined in anhydrous toluene (30 mL) under argon atmosphere in a 250 mL flask. Then, 9-chloro-9-borafluorene (794 mg, 4.0 mmol) dissolved by anhydrous toluene (10 mL) was slowly added to the mixture. The mixture was stirred at 100 °C for 6 h. After cooled to room temperature, the mixture was extracted by dichloromethane and water for three times. The separated organic layer was dried over anhydrous sodium sulfate and the solvent was then removed by rotary evaporation. The crude product was purified by silica gel column chromatography (petroleum ether/dichloromethane=6/1, V/V). **mB-F** was obtained as a red solid. (605 mg, yield 60%). ¹H-NMR (500 MHz, CDCl₃, δ, ppm): 7.67 (d, *J*=3.5 Hz, 4H), 7.49 (s, 2H), 7.45 (m, 4H), 7.31(s, 2H), 7.28 (m, 4H), 7.08 (t, 4H), 3.12 (s, 4H), 1.29 (s, 2H), 1.17(m, 6H), 1.14 (m, 6H), 1.03 (m, 16H), 0.88 (t, 6H), 0.82 (s, 4H), 0.68 (s, 6H). ¹³C-NMR (126 MHz, CDCl₃, δ, ppm): 146.86, 140.12, 135.02, 132.45, 129.96, 125.46, 122.01, 119.38, 115.25, 52.43, 37.78, 31.88, 31.45, 31.09, 29.73, 29.08, 26.86, 23.07, 22.66, 14.08. Anal. Calcd. for C₅₈H₇₀B₂Br₂N₄: C, 69.34; H, 7.02; Br, 2.15; N, 15.91; Found: C, 69.32; H, 6.98; N, 5.57.

Synthesis of **mB-FBu**

5,5'-Dibromo-*N*³,*N*³-bis(2-butyloctyl)-[2,2'-bipyridine]-3,3'-diamine (1) (681 mg, 1.0 mmol) and triethylamine (405 mg, 4.0 mmol) were combined in anhydrous toluene (30 mL) under argon atmosphere in a 250 mL flask. Then, 2,7-di-*tert*-butyl-9-chloro-9-borafluorene (1.24 g, 4.0 mmol) dissolved by anhydrous toluene (10 mL) was slowly added to the mixture. The

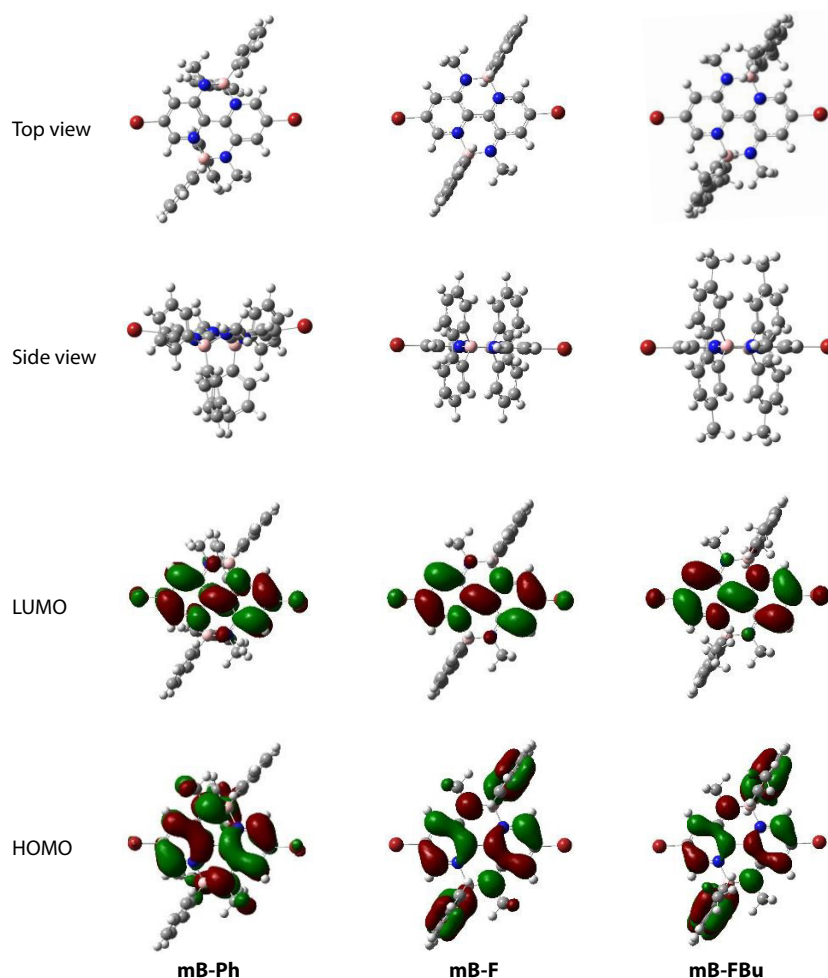


Fig. 1 The optimized geometries and the Kohn-Sham LUMO/HOMOs of **mB-Ph**, **mB-F** and **mB-FBu**.

mixture was stirred at 100 °C for 6 h. After cooled to room temperature, the mixture was extracted by dichloromethane and water for three times. The separated organic layer was dried over anhydrous sodium sulfate and the solvent was then removed by rotary evaporation. The crude product was purified by silica gel column chromatography (petroleum ether/dichloromethane=8/1, V/V). **mB-FBu** was obtained as a red solid. (762 mg, yield 62%). $^1\text{H-NMR}$ (500 MHz, C_6D_6 , δ , ppm) 7.94 (s, 2H), 7.66 (m, 4H), 7.52–7.43 (m, 6H), 7.39–7.31 (m, 4H), 2.99 (d, $J=7.2$ Hz, 4H), 1.48–1.43 (m, 2H), 1.25 (t, $J=8.8$ Hz, 36H), 1.13 (dd, $J=14.7$, 6.5 Hz, 5H), 1.07–1.02 (m, 10H), 1.00–0.93 (m, 9H), 0.91–0.86 (m, 13H), 0.78 (t, $J=7.3$ Hz, 6H). $^{13}\text{C-NMR}$ (126 MHz, C_6D_6 , δ , ppm): 149.55, 148.77, 146.93, 146.79, 146.66, 131.10, 129.41, 125.68, 125.50, 121.76, 119.44, 52.14, 36.54, 34.44, 32.56, 32.26, 31.89, 31.38, 29.73, 28.96, 26.87, 23.06, 22.74, 14.03, 13.89. Anal. Calcd. for $\text{C}_{74}\text{H}_{102}\text{B}_2\text{Br}_2\text{N}_4$: C, 72.32; H, 8.37; Br, 1.76; N, 4.56. Found: C, 72.28; H, 8.36; N, 4.55.

Synthesis of **PB-Ph**

Bis(1,5-cyclooctadiene)nickel(0) (127.0 mg, 0.45 mmol), 2,2'-bipyridine (70.3 mg, 0.45 mmol) and 1,5-cyclooctadiene (56 μL , 0.45 mmol) were placed in a two-necked flask under argon. Dried toluene (20 mL) was then added. After the mixture being stirred at 80 °C for 30 min, monomer **mB-Ph** (110.8 mg, 0.11 mmol) was dissolved in toluene (10 mL) and added into the flask

dropwise. End-capping reaction was carried out by adding bromobenzene (50.0 mg, 0.32 mmol) after 4 h. The resulting organic phase was dispersed in acetonitrile and the precipitate was collected. The precipitate was purified by Soxhlet extraction in acetone, hexane and chloroform. The solid from the hexane solution was dispersed in acetonitrile, then collected and dried in vacuum overnight. Homopolymer **PB-Ph** was obtained as a red solid (80.6 mg, yield 95%). GPC (TCB, polystyrene standard, 150 °C): $M_n=25.8$ kDa, PDI=2.03. Anal. Calcd. for $\text{C}_{58}\text{H}_{74}\text{B}_2\text{N}_4$: C, 82.07; H, 8.79; B, 2.55; N, 6.60. Found: C, 82.04; H, 8.77; N, 6.59.

Synthesis of **PB-F**

PB-F was prepared from compound **mB-F** (100.0 mg, 0.10 mmol) in a procedure similar to that of **PB-Ph**. The polymer **PB-F** was obtained as a dark blue solid (74.5 mg, yield 88%). GPC (TCB, polystyrene standard, 150 °C): $M_n=44.0$ kDa, PDI=1.85. Anal. Calcd. for $\text{C}_{58}\text{H}_{72}\text{B}_2\text{N}_4$: C, 82.46; H, 8.35; B, 2.56; N, 6.63. Found: C, 82.43; H, 8.29; N, 6.61.

Synthesis of **PB-FBu**

PB-FBu was prepared from compound **mB-FBu** (123.0 mg, 0.10 mmol) in a procedure similar to that of **PB-Ph**. The polymer **PB-FBu** was obtained as a dark blue solid (87.7 mg, yield 82%). GPC (TCB, polystyrene standard, 150 °C): $M_n=25.2$ kDa, PDI=2.11. Anal. Calcd. for $\text{C}_{74}\text{H}_{102}\text{B}_2\text{N}_4$: C, 83.12; H, 9.62; B, 2.02; N, 5.24. Found: C, 83.09; H, 9.60; N, 5.22.

RESULTS AND DISCUSSION

Synthesis and Characterization

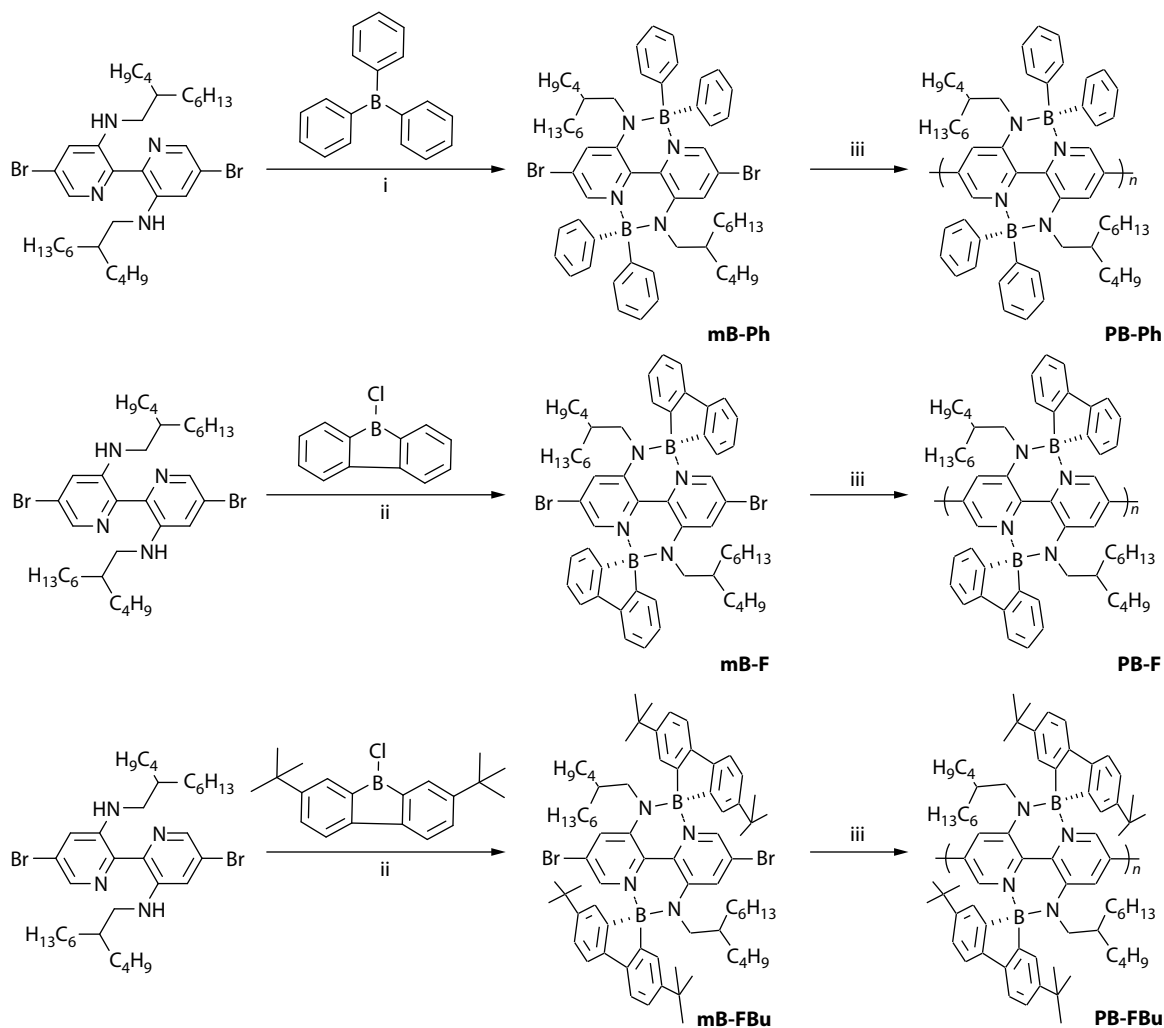
Scheme 2 displays the synthetic routes to the three monomers **mB-Ph**, **mB-F**, **mB-FBu** and three homopolymers **PB-Ph**, **PB-F**, **PB-FBu**. The starting materials, 5,5'-dibromo-*N*³,*N*^{3'}-di-2-butyl-octyl-[2,2'-bipyridine]-3,3'-diamine (1), triphenylboron, 9-chloro-9-borofluorene and 2,7-di-*tert*-butyl-9-chloro-9-borofluorene were synthesized following the previously reported methods.^[36–38] The three monomers were prepared by the borylation of (1) with triphenylboron, 9-chloro-9-borofluorene and 2,7-di-*tert*-butyl-9-chloro-9-borofluorene, respectively. The synthesis of **mB-F** and **mB-FBu** differs from that of **mB-Ph**. NEt₃ is added to neutralise the HCl produced in the reaction, allowing the reaction to proceed positively. The three homopolymers **PB-Ph**, **PB-F** and **PB-FBu** were obtained by Yamamoto polymerization of three monomers.

The chemical structures of the three monomers and the three polymers were confirmed by ¹H-NMR, ¹³C-NMR and elemental analysis. As determined by gel permeation chromatography (GPC), the number-average molecular weight

(*M*_n) and polydispersity index (PDI) are 25.8 kDa and 2.03 for **PB-Ph**, 44.0 kDa and 1.94 for **PB-F**, 25.2 kDa and 2.11 for **PB-FBu**, respectively. All the three polymers are readily soluble in common organic solvents, such as chloroform, toluene, chlorobenzene, etc. As indicated by thermogravimetric analysis (TGA) in a nitrogen atmosphere, the three polymers all exhibit excellent thermal stability with thermal degradation temperature at 5% weight loss of higher than 320 °C (Fig. S8 in ESI).

Optoelectronic Properties of the Monomers

UV-Vis absorption, fluorescence spectra and phosphorescence spectra of the three monomers, are shown in Figs. 2(a)–2(c), respectively. The characteristics are summarized in Table 1. **mB-Ph**, **mB-F** and **mB-FBu** show the maximum absorption wavelength of 549, 566 and 580 nm, respectively. The peak fluorescence wavelength of **mB-Ph**, **mB-F** and **mB-FBu** is 594, 602 and 614 nm, respectively, indicating the Stokes shifts of 45, 36 and 34 nm, respectively. Compared to **mB-Ph**, **mB-F** with borofluorene substituent group and **mB-FBu** with *tert*-butyl groups on the borofluorene exhibit progressively red-shifted absorption and fluorescence spectra. These results indicate that the substi-



Scheme 2 Synthetic routes to **PB-Ph**, **PB-F** and **PB-FBu**. Reagents and conditions: (i) Toluene, 120 °C; (ii) Triethylamine, toluene, 90 °C; (iii) Bis(1,5-cyclooctadiene)nickel(0), 2,2'-bipyridine, 1,5-cyclooctadiene, toluene, 80 °C.

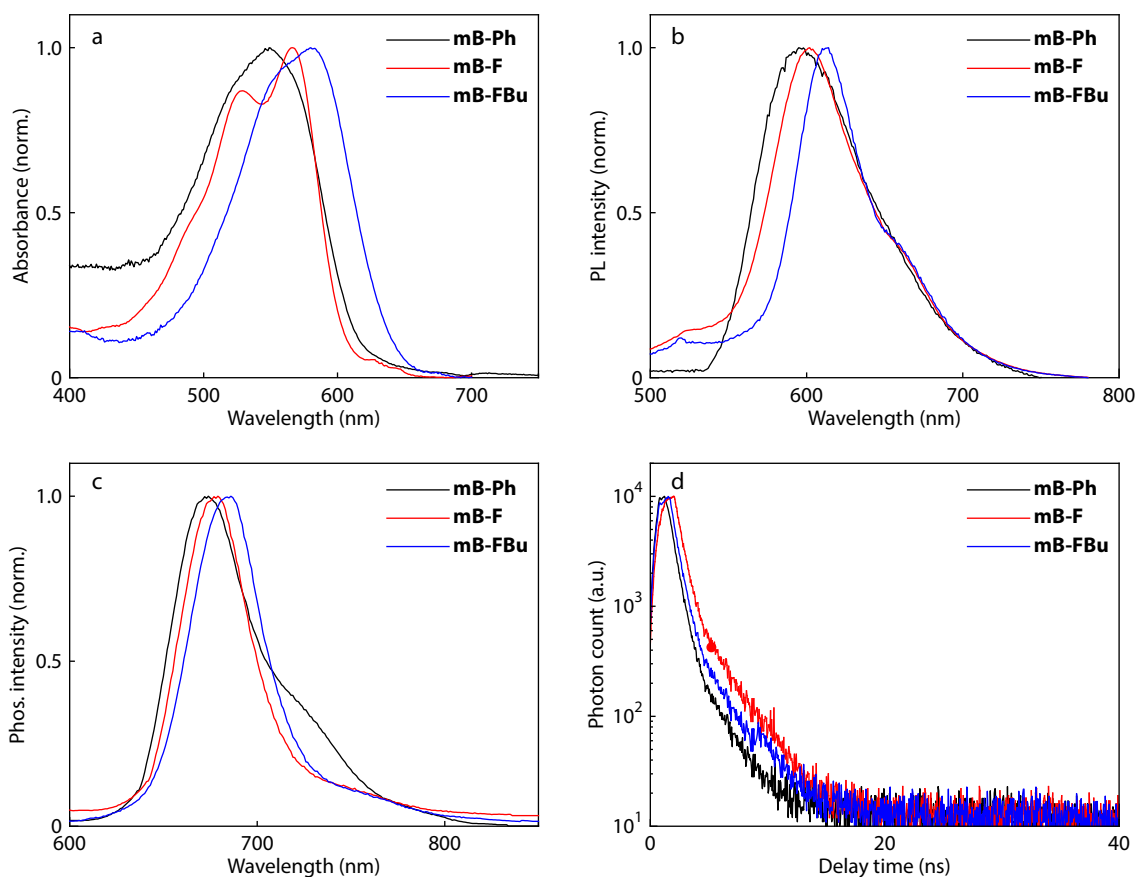


Fig. 2 (a) UV-Vis absorption spectra and (b) fluorescence spectra of **mB-Ph**, **mB-F** and **mB-FBu** in dichloromethane solution; (c) Phosphorescence spectra of **mB-Ph**, **mB-F** and **mB-FBu** in dichloromethane solution at $-196\text{ }^{\circ}\text{C}$; (d) The transient PL spectra of **mB-Ph**, **mB-F** and **mB-FBu** in toluene.

Table 1 Photophysical and electrochemical characteristics of **mB-Ph**, **mB-F** and **mB-FBu**.

Sample	$\lambda_{\text{Abs}}^{\text{sol a}}$ (nm)	$\lambda_{\text{Abs}}^{\text{film b}}$ (nm)	$\lambda_{\text{PL}}^{\text{sol a}}$ (nm)	$\lambda_{\text{PL}}^{\text{film b}}$ (nm)	$E_{\text{S}}/E_{\text{T}}^{\text{c}}$ (eV)	$\Delta E_{\text{ST}}^{\text{d}}$ (eV)	FWHM ^b (nm)	$\Phi_{\text{PL}}^{\text{a}}$ (%)	$\tau_{\text{p}}^{\text{[e]}}$ (ns)	$E_{\text{LUMO}}^{\text{f}}$ (eV)	$E_{\text{HOMO}}^{\text{f}}$ (eV)	$E_{\text{g}}^{\text{opt b}}$ (eV)
mB-Ph	549	560	594	607	2.21/1.97	0.24	84	83	3.45	-3.19	-5.49	2.03
mB-F	566	570	602	612	2.20/1.97	0.23	67	88	7.22	-3.20	-5.38	2.02
mB-FBu	580	584	614	620	2.14/1.92	0.22	49	86	4.88	-3.10	-5.19	1.99

^a Measured in dichloromethane solution at a concentration of 1×10^{-5} mol/L; ^b Measured in thin film; ^c The lowest singlet and triplet states energy level; ^d $\Delta E_{\text{ST}} = S_1 - T_1$; ^e Prompt fluorescence lifetime estimated from the transient PL in toluene at a concentration of 1×10^{-5} mol/L, which were measured under nitrogen atmosphere at room temperature with an excitation of 550 nm; ^f Estimated based on the onset oxidation and reduction potentials in CV, $E_{\text{HOMO}}/E_{\text{LUMO}} = -(4.80 + E_{\text{onset}}^{\text{ox}}/E_{\text{onset}}^{\text{red}})$ eV.

tutes on the boron atoms can obviously affect the opto-electronic properties of the BNPB building blocks. **mB-Ph**, **mB-F** and **mB-FBu** show the maximum phosphorescence wavelength of 674, 679 and 686 nm. The singlet-triplet energy splitting (ΔE_{ST}) of all the three monomers is estimated to be as small as ca. 0.23 eV. However, despite the small ΔE_{ST} , all the three monomers exhibit fluorescence lifetime of less than 10 ns (Fig. 2d) with no thermally assist delayed fluorescence. The ΔE_{ST} of these three monomers may not be small enough compared to the efficient TADF molecular systems.

Fig. S1(c) (in ESI) shows the cyclic voltammograms (CV) of **mB-Ph**, **mB-F** and **mB-FBu** in CH_2Cl_2 solution. All the three monomers exhibit obvious reduction and oxidation waves. According to the onset reduction and oxidation potentials, the LUMO/HOMO energy levels of **mB-Ph**, **mB-F** and **mB-FBu**

are estimated to be $-3.19/-5.49$, $-3.20/-5.38$ and $-3.10/-5.19$ eV, respectively. Compared to **mB-Ph**, **mB-F** exhibits a similar LUMO energy level but a slightly upshifted HOMO energy level, suggesting a slightly decreased bandgap. This is consistent with the slightly red-shifted absorption spectra of **mB-F** than that of **mB-Ph**. **mB-FBu** shows both upshifted LUMO energy levels and HOMO energy levels than that of **mB-F** because of the electron-donating property of *tert*-butyl groups.

Optoelectronic Properties of the Polymers

Fig. 3(a) shows the absorption spectra of the three polymers, **PB-Ph**, **PB-F** and **PB-FBu**, in dilute dichloromethane solution. The characteristics are listed in Table 2. **PB-Ph**, **PB-F** and **PB-FBu** show the maximum absorption wavelength of 618, 662 and 670 nm, respectively. According to the onset absorption wave-

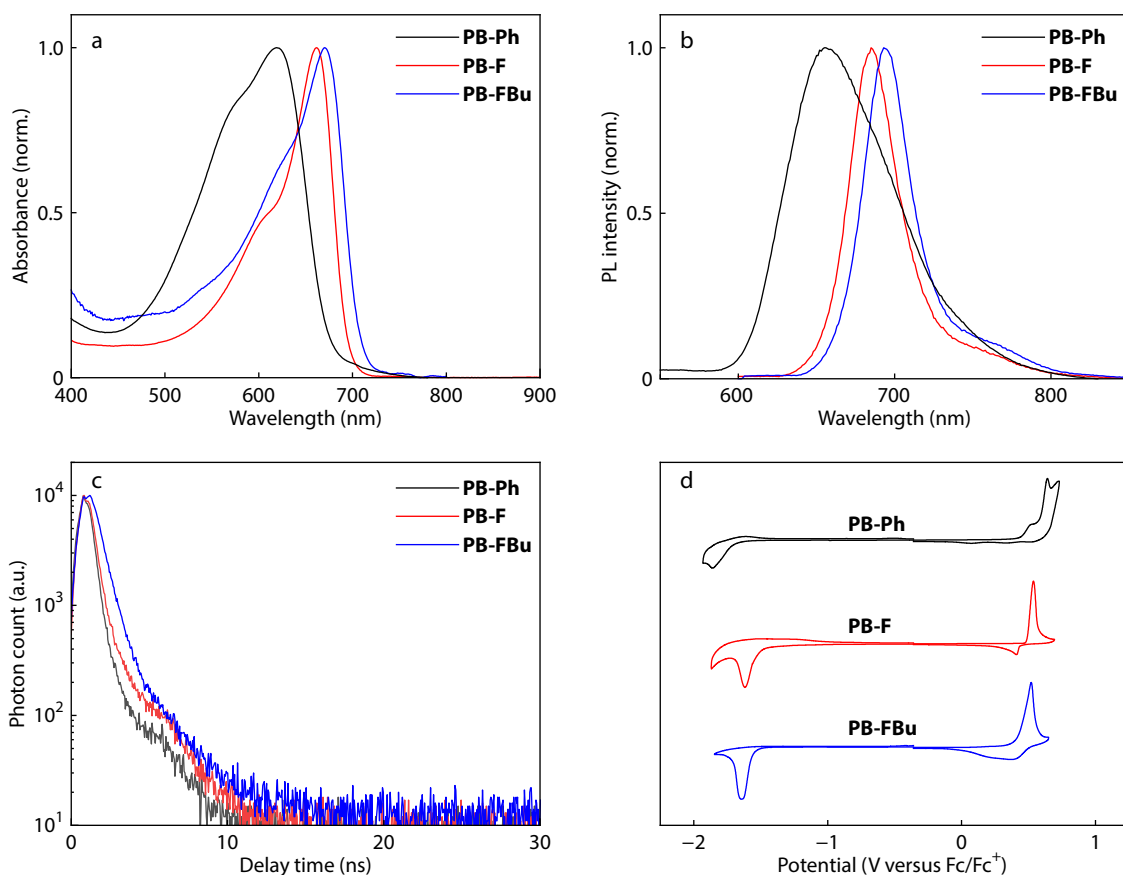


Fig. 3 (a) UV-Vis absorption spectra, (b) fluorescence spectra and (c) the transient PL spectra of **PB-Ph**, **PB-F** and **PB-FBu** in dichloromethane; (d) Cyclic voltammograms of **PB-Ph**, **PB-F** and **PB-FBu** in the thin film.

Table 2 Photophysical and electrochemical characteristics of **PB-Ph**, **PB-F** and **PB-FBu**.

Sample	$\lambda_{\text{Abs}}^{\text{sol a}}$ (nm)	$\lambda_{\text{Abs}}^{\text{film b}}$ (nm)	$\lambda_{\text{PL}}^{\text{sol a}}$ (nm)	$\lambda_{\text{PL}}^{\text{film b}}$ (nm)	FWHM ^b (nm)	$\Phi_{\text{sol}}^{\text{a}}$ (%)	$\Phi_{\text{film}}^{\text{b}}$ (%)	$\tau_{\text{p}}^{\text{c}}$ (ns)	$E_{\text{LUMO}}^{\text{b}}$ (eV)	$E_{\text{HOMO}}^{\text{b}}$ (eV)	$E_{\text{g}}^{\text{opt b}}$ (eV)
PB-Ph	618	630	656	668	79	63	14	1.35	-3.11	-5.24	1.80
PB-F	662	669	682	700	39	71	16	1.61	-3.27	-5.27	1.72
PB-FBu	670	678	693	709	37	69	12	2.22	-3.22	-5.21	1.71

^a Measured in dichloromethane solution at a concentration of 1×10^{-5} mol/L; ^b Measured in thin film; ^c Prompt fluorescence lifetimes estimated from the transient PL in toluene at a concentration of 1×10^{-5} mol/L, which were measured under nitrogen atmosphere at room temperature with an excitation of 550 nm.

length in thin film (Fig. S4a in ESI), the optical bandgap of **PB-Ph**, **PB-F** and **PB-FBu** are estimated to be 1.80, 1.72 and 1.70 eV, respectively. Fig. 3(b) shows the fluorescence spectra of the three polymers. **PB-Ph**, **PB-F** and **PB-FBu** in solution emit deep-red light with the maximum emission wavelength of 656, 682 and 693 nm, respectively, together with the full width at half maximum (FWHM) of 79, 39 and 37 nm, respectively. It is worth noting that the FWHM of **PB-Ph** is much wider than those of the other two polymers. This is probably due to the rotatable phenyl groups which increase the non-radiative energy loss. Obviously, the more red-shifted fluorescence spectrum of the monomer, the more red-shifted fluorescence spectra of the homopolymers. The fluorescence spectra of **PB-F** and **PB-FBu** is much narrower than that of **PB-Ph** probably because the borafluorene unit is more rigid than the diphenylboron unit. The rigid polymer backbone and aromatic substitutes suppress molecular rotation and vibration, leading to a narrow emission spec-

trum. The three homopolymers all exhibit high fluorescence quantum efficiency of exceeding 0.60, which has not been reported for red light-emitting conjugated homopolymers, e.g., polythiophene derivatives. The fluorescence quantum efficiency of **PB-F**, **PB-FBu** is even higher than that of **PB-Ph** probably due to the rigid polymer backbones. To estimate the LUMO/HOMO energy levels of the three polymers, CV measurements of **PB-Ph**, **PB-F** and **PB-FBu** in thin films were performed and the results are shown in Fig. 3(c). All the three polymers exhibit obvious reduction and oxidation waves. According to the onset potentials of the reduction/oxidation waves, the $E_{\text{LUMO}}/E_{\text{HOMO}}$ values of **PB-Ph**, **PB-F** and **PB-FBu** are estimated to be -3.11/-5.24 eV, -3.27/-5.27 eV and -3.20/-5.18 eV (Table 2), respectively.

Electroluminescent Properties

To evaluate the potential of the organoboron conjugated homopolymers as red light-emitting materials, we used them as

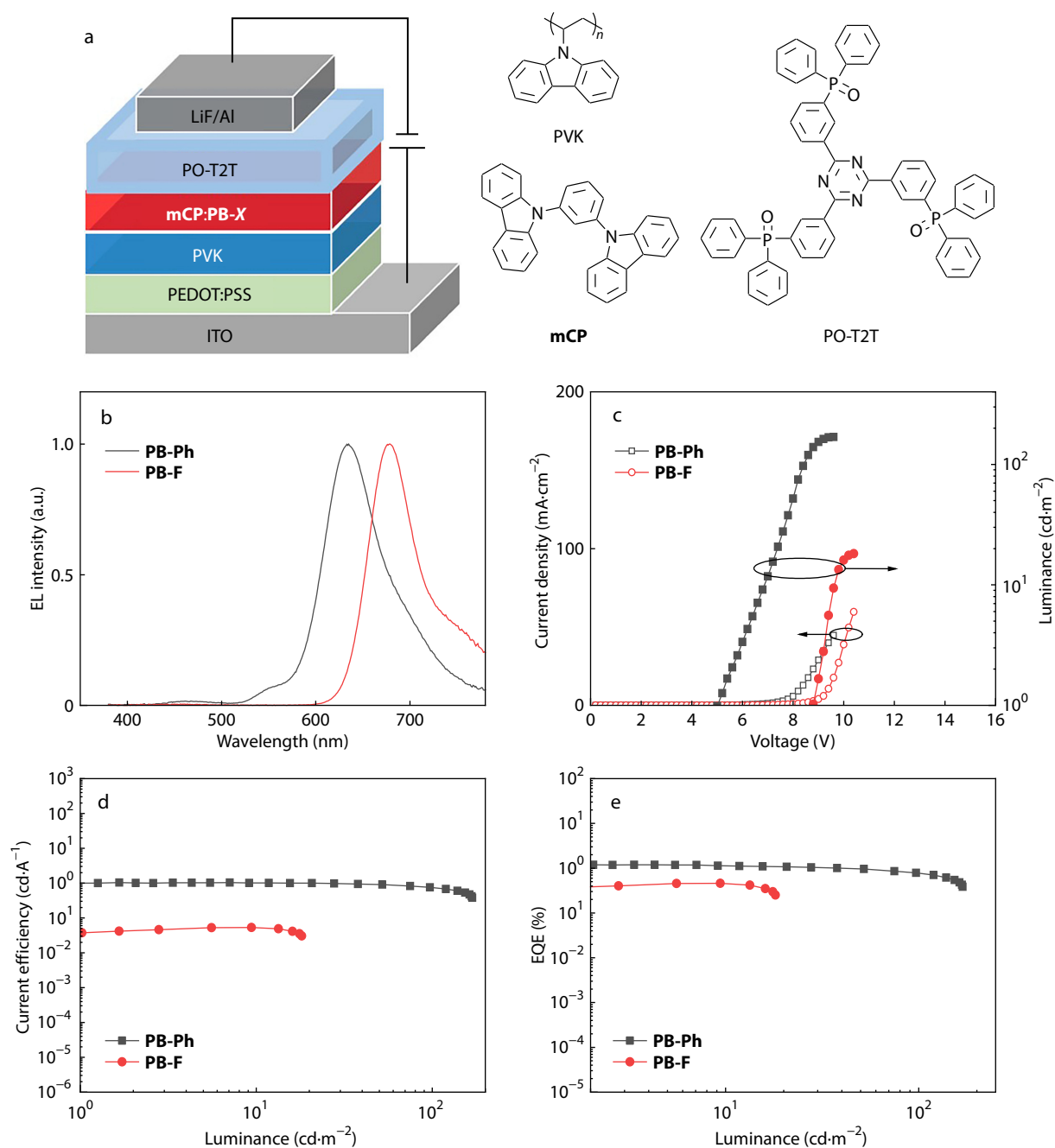


Fig. 4 (a) The device structure of OLED and molecular structures of used materials; (b) EL spectra of **PB-Ph**, **PB-F**; (c) Current density-voltage-luminance curves of OLED; (d) Current efficiency-luminance curves of OLED; (e) Power efficiency-luminance curves of OLED.

the emitters dispersed in a host to fabricate solution-processed OLEDs with the architecture of ITO/poly(3,4-ethylenedioxythiophene):poly(styrenesulfonate) (PEDOT:PSS) (40 nm)/poly(vinyl carbazole) (PVK) (30 nm)/EML (50 nm)/1,3,5-triazine-2,4,6-triyl-tris(benzene-3,1-diyl)-tris(diphenylphosphine oxide) (PO-T2T) (50 nm)/LiF (1 nm)/Al (150 nm) (Fig. 4a). PEDOT:PSS and PVK are used as the hole-injection layer and hole transporting layer, respectively. PO-T2T serves as the electron-transporting layer and 1,3-bis(carbazol-9-yl)benzene (mCP) works as the host. The **PB-Ph**, **PB-F** are dispersed in mCP with a ratio of 4 wt% to form the emitting layer. The PLQYs of **PB-Ph** and **PB-F** in the emitting layer show moderate values of 0.22 and 0.19, respectively. Table

3 lists the characteristics of the two solution-processed OLED devices. The device of **PB-Ph** emits pure red light with the Commission International de l'Eclairage (CIE) coordinates of (0.63, 0.35). It shows a maximum current efficiency of 1.00 cd·A⁻¹, a maximum power efficiency of 0.60 lm·W⁻¹, a maximum external quantum efficiency (EQE) of 1.20% and a turn-on voltage of 5.0 V, a maximum luminance of 169 cd·m⁻². This performance is fairly comparable to that of typical red fluorescent polymers but is inferior to those of red phosphorescent polymers and red TADF polymers.^[39–45] The OLED device efficiency of **PB-F** is lower than that of **PB-Ph** probably because of the unbalanced charge carrier injection/transporting. The turn on voltage of the

Table 3 Summary of device performance.

Device	V_{on}^a (V)	L^b ($cd\cdot m^{-2}$)	CE ^b ($cd\cdot A^{-1}$)	PE ^b ($lm\cdot W^{-1}$)	EQE ^b (%)	CIE ^b (x, y)
mCP:PB-Ph	5.0	169	1.00	0.60	1.20	(0.63, 0.35)
mCP:PB-F	8.7	18	0.05	0.02	0.46	(0.69, 0.27)

^a Turn-on voltage at $1\text{ cd}\cdot\text{m}^{-2}$; ^b Max performance; CE: current efficiency; PE: power efficiency; EQE: external quantum efficiency.

OLED device of **PB-F** is higher than that of the device of **PB-Ph**. This is probably due to the serious charge trapping effect of the deep-red light emitting polymers in the mCP host.^[46,47] For the polymer PB-FPO, we did not fabricate OLED devices due to the relatively low fluorescence quantum efficiency.

CONCLUSIONS

In summary, we developed a series of organoboron conjugated homopolymers based on BNPB unit with deep-red emission. The three homopolymers show pure red or deep red-light emission with high fluorescence quantum efficiency, which is attributed to the rigid backbone and large steric hindrance. The polymers have been used as the emitters in solution processed OLEDs with decent device performance. This work indicates a new strategy to design highly efficient light emitting conjugated polymers.

Conflict of Interests

The authors declare no interest conflict.

Electronic Supplementary Information

Electronic supplementary information (ESI) is available free of charge in the online version of this article at <http://doi.org/10.1007/s10118-024-3123-7>.

Data Availability Statement

The related data (DOI: 10.57760/sciencedb.j00189.00021) for this paper is available in the Data Repository of China Association for Science and Technology (<https://www.scidb.cn/c/cjps>).

ACKNOWLEDGMENTS

This work was financially supported by the National Natural Science Foundation of China (Nos. 22135007 and 52073281).

REFERENCES

- Burroughes, J. H.; Bradley, D. D. C.; Brown, A. R.; Marks, R. N.; Mackay, K.; Friend, R. H.; Burns, P. L.; Holmes, A. B. Light-emitting diodes based on conjugated polymers. *Nature* **1990**, *347*, 539–541.
- Heeger, A. J. Semiconducting and metallic polymers: the fourth generation of polymeric materials (Nobel Lecture). *Angew. Chem. Int. Ed.* **2001**, *40*, 2591–2611.
- Wang, Z. B.; Helander, M. G.; Qiu, J.; Puzzo, D. P.; Greiner, M. T.; Hudson, Z. M.; Wang, S.; Liu, Z. W.; Lu, Z. H. Unlocking the full potential of organic light-emitting diodes on flexible plastic. *Nat.*

Photon. **2011**, *5*, 753–757.

- Guo, X.; Baumgarten, M.; Müllen, K. Designing π -conjugated polymers for organic electronics. *Prog. Polym. Sci.* **2013**, *38*, 1832–1908.
- Huang, W. Polymers for flexible electronics. *Chinese J. Polym. Sci.* **2022**, *40*, 1513–1514.
- Murto, P.; Minotto, A.; Zampetti, A.; Xu, X.; Andersson, M. R.; Cacialli, F.; Wang, E. Triazolobenzothiadiazole-based copolymers for polymer light-emitting diodes: pure near-infrared emission via optimized energy and charge transfer. *Adv. Opt. Mater.* **2016**, *4*, 2068–2076.
- Ostroverkhova, O. Organic optoelectronic materials: mechanisms and applications. *Chem. Rev.* **2016**, *116*, 13279–13412.
- Tang, S.; Murto, P.; Xu, X.; Larsen, C.; Wang, E.; Edman, L. Intense and stable near-infrared emission from light-emitting electrochemical cells comprising a metal-free indacenodithieno[3,2-*b*]thiophene-based copolymer as the single emitter. *Chem. Mat.* **2017**, *29*, 7750–7759.
- Bai, L.; Sun, C.; Han, Y.; Wei, C.; An, X.; Sun, L.; Sun, N.; Yu, M.; Zhang, K.; Lin, J.; Xu, M.; Xie, L.; Ling, H.; Cabanillas-Gonzales, J.; Song, L.; Hao, X.; Huang, W. Steric poly(diaryl)fluorene-cobenzothiadiazole for efficient amplified spontaneous emission and polymer light-emitting diodes: benefit from preventing interchain aggregation and polaron formation. *Adv. Opt. Mater.* **2020**, *8*, 1901616.
- Liu, Y.; Hua, L.; Yan, S.; Ren, Z. Halogenated π -conjugated polymeric emitters with thermally activated delayed fluorescence for highly efficient polymer light emitting diodes. *Nano Energy* **2020**, *73*, 104800.
- Gon, M.; Wakabayashi, J.; Nakamura, M.; Tanaka, K.; Chujo, Y. Controlling energy gaps of π -conjugated polymers by multi-fluorinated boron-fused azobenzene acceptors for highly efficient near-infrared emission. *Chem. Asian J.* **2021**, *16*, 696–703.
- Guo, X.; Zhang, Y.; Hu, Y.; Yang, J.; Li, Y.; Ni, Z.; Dong, H.; Hu, W. Molecular weight engineering in high-performance ambipolar emissive mesopolymers. *Angew. Chem. Int. Ed.* **2021**, *60*, 14902–14908.
- Wang, T.; Zou, Y.; Huang, Z.; Li, N.; Miao, J.; Yang, C. Narrowband emissive TADF conjugated polymers towards highly efficient solution-processible OLEDs. *Angew. Chem. Int. Ed.* **2022**, *61*, e202211172.
- Li, X.; Yan, L.; Liu, S.; Wang, S.; Rao, J.; Zhao, L.; Tian, H.; Ding, J.; Wang, L. Polymerized thermally activated delayed-fluorescence small molecules: long-axis polymerization leads to a nearly concentration-independent luminescence. *Angew. Chem. Int. Ed.* **2023**, *62*, e202300529.
- Nakamura, M.; Gon, M.; Tanaka, K.; Chujo, Y. Solid-state near-infrared emission of π -conjugated polymers consisting of boron complexes with vertically projected steric substituents. *Macromolecules* **2023**, *56*, 2709–2718.
- He, Z. W.; Zhang, Q.; Li, C. X.; Han, H. T.; Lu, Y. Synthesis of thieno[3,4-*b*]pyrazine-based alternating conjugated polymers via direct arylation for near-infrared OLED applications. *Chinese J. Polym. Sci.* **2022**, *40*, 138–146.
- Pei, Q.; Yang, Y. Efficient photoluminescence and electroluminescence from a soluble polyfluorene. *J. Am. Chem. Soc.* **1996**, *118*, 7416–7417.
- Grell, M.; Bradley, D. D. C.; Ungar, G.; Hill, J.; Whitehead, K. S.

- Interplay of physical structure and photophysics for a liquid crystalline polyfluorene. *Macromolecules* **1999**, *32*, 5810–5817.
- 19 Bernius, M. T.; Inbasekaran, M.; O'Brien, J.; Wu, W. Progress with light-emitting polymers. *Adv. Mater.* **2000**, *12*, 1737–1750.
- 20 Leclerc, M. Polyfluorenes: twenty years of progress. *J. Polym. Sci., Part A: Polym. Chem.* **2001**, *39*, 2867–2873.
- 21 List, E. J. W.; Guentner, R.; Scanducci de Freitas, P.; Scherf, U. The effect of Keto defect sites on the emission properties of polyfluorene-type materials. *Adv. Mater.* **2002**, *14*, 374–378.
- 22 Wang, M.; Li, Y.; Xie, Z.; Wang, L. Polyfluorenes containing pyrazine units: synthesis, photophysics and electroluminescence. *Sci. China Chem.* **2011**, *54*, 656–665.
- 23 Sun, M. L.; Zhong, C. M.; Li, F.; Pei, Q. B. Purified polar polyfluorene for light-emitting diodes and light-emitting electrochemical cells. *Chinese J. Polym. Sci.* **2012**, *30*, 503–510.
- 24 Braun, D.; Gustafsson, G.; McBranch, D.; Heeger, A. J. Electroluminescence and electrical transport in poly(3-octylthiophene) diodes. *J. Appl. Phys.* **1992**, *72*, 564–568.
- 25 Ruseckas, A.; Namdas, E. B.; Theander, M.; Svensson, M.; Yartsev, A.; Zigmantas, D.; Andersson, M. R.; Inganäs, O.; Sundström, V. Luminescence quenching by inter-chain aggregates in substituted polythiophenes. *J. Photochem. Photobiol. A-Chem.* **2001**, *144*, 3–12.
- 26 Brown, P. J.; Thomas, D. S.; Köhler, A.; Wilson, J. S.; Kim, J.-S.; Ramsdale, C. M.; Siringhaus, H.; Friend, R. H. Effect of interchain interactions on the absorption and emission of poly(3-hexylthiophene). *Phys. Rev. B* **2003**, *67*, 064203.
- 27 Barbarella, G.; Melucci, M.; Sotgiu, G. The versatile thiophene: an overview of recent research on thiophene-based materials. *Adv. Mater.* **2005**, *17*, 1581–1593.
- 28 Dou, C.; Long, X.; Ding, Z.; Xie, Z.; Liu, J.; Wang, L. An electron-deficient building block based on the B←N Unit: an electron acceptor for all-polymer solar cells. *Angew. Chem. Int. Ed.* **2016**, *55*, 1436–1440.
- 29 Long, X.; Ding, Z.; Dou, C.; Zhang, J.; Liu, J.; Wang, L. Polymer acceptor based on double B←N bridged bipyridine (BNBP) unit for high-efficiency all-polymer solar cells. *Adv. Mater.* **2016**, *28*, 6504–6508.
- 30 Zhang, Z.; Miao, J.; Ding, Z.; Kan, B.; Lin, B.; Wan, X.; Ma, W.; Chen, Y.; Long, X.; Dou, C.; Zhang, J.; Liu, J.; Wang, L. Efficient and thermally stable organic solar cells based on small molecule donor and polymer acceptor. *Nat. Commun.* **2019**, *10*, 3271.
- 31 Zhao, R.; Wang, N.; Yu, Y.; Liu, J. Organoboron polymer for 10% efficiency all-polymer solar cells. *Chem. Mat.* **2020**, *32*, 1308–1314.
- 32 Cao, X.; Li, H.; Hu, J.; Tian, H.; Han, Y.; Meng, B.; Liu, J.; Wang, L. An amorphous n-type conjugated polymer with an ultra-rigid planar backbone. *Angew. Chem. Int. Ed.* **2023**, *62*, e202212979.
- 33 Dong, C.; Deng, S.; Meng, B.; Liu, J.; Wang, L. A distannylated monomer of a strong electron-accepting organoboron building block: enabling acceptor-acceptor-type conjugated polymers for n-type thermoelectric applications. *Angew. Chem. Int. Ed.* **2021**, *60*, 16184–16190.
- 34 Wang, J.; Zhao, R.; Zhang, L.; Miao, J.; Liu, J.; Wang, L. A Direct surface modification strategy of ITO anodes enables high-performance organic photodetectors. *J. Mater. Chem. C* **2023**, *11*, 14421–14428.
- 35 Long, X.; Li, D.; Wang, B.; Jiang, Z.; Xu, W.; Wang, B.; Yang, D.; Xia, Y. Heterocyclization strategy for construction of linear conjugated polymers: efficient metal-free electrocatalysts for oxygen reduction. *Angew. Chem. Int. Ed.* **2019**, *58*, 11369–11373.
- 36 Hübner, A.; Diefenbach, M.; Bolte, M.; Lerner, H. W.; Holthausen, M. C.; Wagner, M. Confirmation of an early postulate: B-C-B two-electron-three-center bonding in organo(hydro)boranes. *Angew. Chem. Int. Ed.* **2012**, *51*, 12514–12518.
- 37 Müller, M.; Maichle-Mössmer, C.; Bettinger, H. F. BN-phenanthryne: cyclotramerization of an 1,2-azaborine derivative. *Angew. Chem. Int. Ed.* **2014**, *53*, 9380–9383.
- 38 Liu, Q.; Yang, L.; Yao, C.; Geng, J.; Wu, Y.; Hu, X. Controlling the lewis acidity and polymerizing effectively prevent frustrated lewis pairs from deactivation in the hydrogenation of terminal alkynes. *Org. Lett.* **2021**, *23*, 3685–3690.
- 39 Müller, C. D.; Falcou, A.; Reckefuss, N.; Rojahn, M.; Wiederhirn, V.; Rudati, P.; Frohne, H.; Nuyken, O.; Becker, H.; Meerholz, K. Multi-colour organic light-emitting displays by solution processing. *Nature* **2003**, *421*, 829–833.
- 40 Li, B.; Xu, X.; Sun, M.; Fu, Y.; Yu, G.; Liu, Y.; Bo, Z. Porphyrin-cored star polymers as efficient nondoped red light-emitting materials. *Macromolecules* **2006**, *39*, 456–461.
- 41 Qu, B.; Chen, Z.; Liu, Y.; Cao, H.; Xu, S.; Cao, S.; Lan, Z.; Wang, Z.; Gong, Q. Orange and red emitting OLEDs based on phenothiazine polymers. *J. Phys. D: Appl. Phys.* **2006**, *39*, 2680.
- 42 Gather, M. C.; Köhnen, A.; Falcou, A.; Becker, H.; Meerholz, K. Solution-processed full-color polymer organic light-emitting diode displays fabricated by direct photolithography. *Adv. Funct. Mater.* **2007**, *17*, 191–200.
- 43 Wang, T.; Li, K.; Yao, B.; Chen, Y.; Zhan, H.; Xie, Z.; Xie, G.; Yi, X.; Cheng, Y. Rigidity and polymerization amplified red thermally activated delayed fluorescence polymers for constructing red and single-emissive-layer white OLEDs. *Adv. Funct. Mater.* **2020**, *30*, 2002493.
- 44 Fan, Q.; Liu, Y.; Hao, Z.; Li, C.; Wang, Y.; Tan, H.; Zhu, W.; Cao, Y. Polymer light-emitting devices based on europium(III) complex with 11-bromo-dipyrido[3,2-a:2',3'-c]phenazine. *Sci. China Chem.* **2015**, *58*, 1152–1158.
- 45 Chen, L. L.; Peng, L.; Wang, L. Y.; Zhu, X. H.; Zou, J. H.; Peng, J. Molecular engineering of an electron-transport triarylphosphine oxide-triazine conjugate toward high-performance phosphorescent organic light-emitting diodes with remarkable stability. *Sci. China Chem.* **2020**, *63*, 904–910.
- 46 Tao, Y.; Yang, C.; Qin, J. Organic host materials for phosphorescent organic light-emitting diodes. *Chem. Soc. Rev.* **2011**, *40*, 2943–2970.
- 47 Yook, K. S.; Lee, J. Y. Small molecule host materials for solution processed phosphorescent organic light-emitting diodes. *Adv. Mater.* **2014**, *26*, 4218–4233.